Active electrospun nanofibers as an effective reinforcement for highly conducting and durable proton exchange membranes

Rakhi Sood, Stefano Giancola, Anna Donnadio, Marta Zatoń, Nicolas Donzel, Jacques Roziere, Deborah Jones, Sara Cavaliere

Active Electrospun Nanofibers as an Effective Reinforcement for Highly Conducting and Durable Proton Exchange Membranes

Rakhi Sood[1, §], Stefano Giancola[1, §, †], Anna Donnadio[1, ‡], Marta Zatoń[1], Nicolas Donzel[1], Jacques Rozière[1], Deborah J. Jones[1], Sara Cavaliere[1, 2, *]

[1] ICGM Université de Montpellier, CNRS, ENSCM, 34095 Montpellier Cedex 5, France.

[2] Institut Universitaire de France (IUF), Paris, France

[†] present address: Institute of Chemical Research of Catalonia (ICIQ), The Barcelona Institute of Science and Technology (BIST), Tarragona, 43007, Spain.

[‡] present address: Department of Pharmaceutical Sciences - University of Perugia, Via del Liceo 1 - 06123 Perugia, Italy

[§] These authors contributed equally

* Corresponding author: sara.cavaliere@umontpellier.fr, Tel.: +33 4 67 14 90 98

ABSTRACT

Mechanical reinforcement of proton exchange membranes is a great challenge allowing the reduction of their thickness, with the advantages of lower resistance, improved water transport, decreased fuel crossover and high durability, which are crucial for fuel cells. We describe herein a new class of reinforced membranes based on nanofibers of polysulfone (PSU) functionalized with 4-heptyl-1,2,3-triazole (PSUT) likely interacting *via* hydrogen bonds or ionic cross-linking with a short-side-chain type perfluorosulfonic acid (Aquivion®) matrix. PSUT with two functionalization degrees was electrospun into webs which were impregnated with Aquivion® to afford composite membranes that presented higher dimensional stability in water, increased mechanical strength and Young modulus in comparison to reinforced membranes of non-functionalized PSU and pristine ionomer membrane, without any decrease in proton conductivity. Membrane-electrode assemblies incorporating an Aquivion® membrane reinforced with PSUT exhibited 5 times superior durability than those with a pristine Aquivion® membrane without any radical scavenger. These features may be ascribed to the specific interaction between basic fibers and acidic

ionomer. The incorporation of webs of active fibers in ionomer membranes is an effective strategy of reinforcement leading to high performance and increased durability, which can be extended to other kinds of ion exchange membranes and devices.

Keywords:

Proton exchange membrane fuel cell, reinforced membrane, active fibrous reinforcement, electrospinning, triazole functionalization

1. Introduction

The development of membranes with low protonic resistance, gas permeability and cost, and high durability is crucial for the widespread adoption of proton exchange membrane fuel cells (PEMFC) for clean energy conversion[1,2]. In order to optimize the performance of PEMFCs, reduction in the resistance of the polymer electrolyte membrane (PEM) *via* reduction of its thickness is widely suggested[3]. However, this approach brings up degradation issues as thin membranes are weaker and more gas permeable and generally exhibit earlier mechanical failure than thicker membranes[4]. Several physical and chemical approaches have been investigated to increase membrane durability[3], including the use of polymer reinforcements[5–8], inorganic scaffolds[9–11], thermal annealing[12,13] and chemical cross-linking[2]. For instance, expanded polytetrafluoroethylene (ePTFE) impregnated with Nafion® or other perfluorosulfonic acids (PFSA) is currently employed in commercial PEMFC membranes for automotive applications (*e.g.* Gore-Select® membrane) with high durability and mechanical properties.[5,7,8]. However, PTFE suffers from mechanical softening at fuel cell operation temperatures, and its good solvent properties for oxygen lead to high gas crossover affecting the membrane stability.

Another strategy to mechanically reinforce ionomer membranes is the incorporation of a macroporous non-woven nanofiber web into the polymer matrix, allowing for the preparation of composite membranes with controlled 3D design and with significantly improved mechanical properties. In this regard, electrospinning has emerged as a versatile technique for the synthesis of robust and highly porous fibrous webs with targeted morphology, controlled fiber diameters and possibility of upscale[14]. Proton exchange membranes reinforced with electrospun nanofibers are possible candidates to disrupt the usual conductivity/durability trade-off and exceed the performance of state-of-the-art membranes[2,15–17]. Pintauro and coworkers pioneered this approach[18–20]. For instance, nanostructured membranes based on electrospun nanofibers of a robust polymer *i.e.* polysulfone (PSU) embedded into PFSA were prepared for fuel cells and water electrolyzers, where rigid nonwoven provide mechanical strength and low hydrogen crossover, and PFSA provide high proton conductivity[18,21].

Inducing specific ionic interactions at the fiber/matrix interface by combining a polymer bearing basic sites with an ionomer bearing sulfonic/phosphonic acid functionalities substantially increases the impact of the nanofiber web on membrane properties[22–26]. Wang *et al.*[22] reported improved stiffness and dimensional stability for membranes based on sulfonated poly(ether ether ketone) (sPEEK) nanofibers embedded into chitosan matrix

attributed to acid-base interactions. Higher proton conductivity was also obtained for the composite PEM with respect to cast sPEEK and chitosan alone. This behavior was ascribed to the resulting ion pairs on the fiber/ionomer interface generating structurally ordered proton-hopping sites. He *et al.*[23] investigated the effect of different interfacial interactions (acid-acid, acid-base, acid-neutral, base-base, base-neutral) on membranes based on poly(vinyl alcohol) (PVA) nanofibers either non-modified or functionalized with $-NH_2$ or $-SO_3H$ embedded into basic chitosan and acidic sPEEK. The acid-base interaction was demonstrated as the most effective in enhancing membrane mechanical properties and conductivity[23]. Furthermore, membranes comprising electrospun polybenzimidazole nanofiber webs impregnated with Aquivion® thereby coupling acid-base ionic interactions along with the scaffolding effect of nanofibers demonstrated exceptional mechanical stability, low gas crossover and high durability upon long-term fuel cell operation[25].

Since the development of copper-catalyzed azide-alkyne cycloaddition (CuAAC) modular ligation[27,28], a large variety of materials containing 1,2,3-triazole groups with advanced macromolecular design (*e.g.* telechelic polymers, block copolymers, dendrimers *etc.*) have been reported[29–34]. However, only a few studies have investigated acid-base blends based on triazole functionalized polymers[35–38]. Acid-base blend membranes based on crosslinked sulfonated poly(arylene ether) and triazole-containing poly(arylene ether sulfone) demonstrated high proton conductivity, mechanical strength and dimensional stability ascribed to the acid-base interaction. In another approach, polysulfone tethered with amino-benzotriazole side-groups was combined with sulfonated poly (ether ether ketone) (sPEEK) to afford an acid-base polymer composite membrane[38], leading to enhanced performance in fuel cell compared with membrane electrode assemblies (MEAs) based on Nafion® and sPEEK.

We earlier reported the synthesis of 1,2,3-triazole-functionalized polysulfone with different aliphatic and aromatic triazole ring substituents *via* microwave assisted-CuAAC[39]. In this work we describe an active reinforcement based on 1,2,3-triazole functionalized nanofibers embedded in PFSA Aquivion®. High chemical stability, antioxidant activity, aromatic character and ability to form hydrogen bonds[40–42] are relevant characteristics of the 1,2,3-triazole group for fuel cell membrane durability, that potentially impact the overall properties of the corresponding composite membranes. Moreover, this flexible approach demonstrates the possibility of modulating membrane properties by adjusting the number and type of triazole moieties[39]. We investigate the effectiveness of the triazole functionality in

strengthening the impact of the polysulfone electrospun non-wovens on the PFSA matrix. Polysulfone modified with different degrees of 4-heptyl-1,2,3-triazole was synthesized by microwave assisted-CuAAC and electrospun. The resulting fibrous webs were impregnated with Aquivion® with EW of 830 g eq^{-1} (Aq830) to prepare nanocomposite acid-base PEMs. The reinforced membranes were characterized for their proton conductivity, mechanical properties and dimensional stability under humidified conditions, and they were integrated into MEAs which were characterized in single fuel cell for their performance and durability.

2. Experimental Section

2.1. Materials

Chlorotrimethylsilane (TMCS, C_3H_9ClSi, ≥ 97.0 %), p-formaldehyde powder ($HO(CH_2O)_nH$, 95 %), tin tetrachloride ($SnCl_4$, 98 %), sodium azide (NaN_3, ≥ 99%), diisopropylethylamine (DIPEA, $[(CH_3)_2CH]_2NC_2H_5$, 99 %), 1-nonyne ($CH_3(CH_2)_6C{\equiv}CH$, 99%), copper(I) iodide triethylphosphite ($CuI{\cdot}P(OEt)_3$, 97 %), N,N,N′,N″,N″-pentamethyldiethylenetriamine (PMDETA, $[(CH_3)_2NCH_2CH_2]_2NCH_3$, 99 %) and all solvents were purchased from Aldrich and used as received. A 24 wt% Aquivion® dispersion in water (EW=830 g eq^{-1}) was purchased from Solvay Specialty Polymers. Bisphenol A polysulfone (PSU) granules (Mn=80 KDa and Mw=102 KDa) were purchased from Goodfellow.

2.2. Synthesis of polysulfone functionalized with 4-heptyl-1,2,3-triazole (PSUT)

Polysulfone (PSU) functionalized with 4-heptyl-1,2,3-triazole **(Figure S1** of Supporting Information, SI) was synthesized with a procedure based on chloromethylation and azidation as earlier reported[39].

The chloromethyl-functionalized polysulfone (PSUCl) with a degree of functionalization of 30 mol% (PSUCl(0.3), 0.89 g) and 90 mol% (PSUCl(0.9), 0.95 g) functional groups per repeat unit presented the following ^{1}H NMR (400 MHz, DMF; ppm) chemical shifts: δ 8.05−6.90 (aromatic backbone), 4.75 (brs, 2H, C***H***$_2$Cl), 1.70 (brs, 6H, C−C**H**$_3$). ^{13}C NMR (100 MHz, DMF; ppm): δ 162.70−118.16 (aromatic backbone), 42.58 (***C***−CH_3), 41.48 (***C***H_2Cl), 30.60 (C−***C***H_3) (**Figure S1**, SI).

The methylazide-functionalized polysulfone PSUAz presented the following ^{1}H NMR (400 MHz, DMF; ppm) chemical shifts: δ 8.05−6.90 (aromatic backbone), 4.46 (brs, 2H, C***H***$_2N_3$),

1.70 (brs, 6H, C–C***H***$_3$). ^{13}C NMR (100 MHz, DMF; ppm): δ 161.82–117.90 (aromatic backbone), 49.75 (***C***H_2N_3), 42.27 (***C***–CH_3), 30.43 (C– ***C***H_3) (**Figure S1**, SI).

For the triazole functionalization, a solution of PSUAz(0.3) (100 mg, 0.062 mmol of azide functionalities), with 1-nonyne (11.5 mg, 0.093 mmol), CuI·P(OEt)$_3$ (2.2 mg, 0.0062 mmol) and DIPEA (8 mg, 0.062 mmol) in DMF (5 mL) reacted under microwaves (Sairem MiniFlow 220SS) (20 W, 120 °C, 30 minutes under constant stirring). The 4-epthyl-1,2,3-triazole-functionalized polysulfone PSUT(30 mol%) (93 mg) was recovered as previously described[39]. An identical procedure was used combining PSUAz(0.9) (100 mg, 0.19 mmol) with 1-nonyne (34.6 mg, 0.28 mmol) yielding PSUT(90 mol%) (105 mg). 1H NMR (400 MHz, DMF; ppm) of PSUT: δ 8.05–6.90 (aromatic backbone), 7.78 (s, 1H, CN=C***H***), 5.58 (brs, 2H, C***H***$_2$N), 2.52 (t, 2H, CNC***H***$_2$CH$_2$CH$_2$CH$_2$CH$_2$CH$_2$CH$_3$), 1.70 (brs, 6H, C– C***H***$_3$), 1.52 (brs, 2H, CNCH$_2$C***H***$_2$CH$_2$CH$_2$CH$_2$CH$_2$CH$_3$), 1.23 (brs, 8H, CNCH$_2$CH$_2$C***H***$_2$C***H***$_2$C***H***$_2$C***H***$_2$CH$_3$), 0.80 (t, 3H, CNCH$_2$CH$_2$CH$_2$CH$_2$CH$_2$CH$_2$C***H***$_3$). ^{13}C NMR (100 MHz, DMF; ppm): δ 162.65–118.15 (aromatic backbone), 148.19 (***C***N=CH), 122.35 CN=***C***H, 48.64 (***C***H_2N), 42.52 (***C***–CH_3), 30.70 (C–***C***H_3), 31.94–29.15 (CNCH$_2$***C***H$_2$***C***H$_2$***C***H$_2$***C***H$_2$CH$_2$CH$_3$), 25.57 (CN***C***H$_2$CH$_2$CH$_2$CH$_2$CH$_2$CH$_2$CH$_3$), 22.73 (CNCH$_2$CH$_2$CH$_2$CH$_2$CH$_2$***C***H$_2$CH$_3$), 13.96 (CNCH$_2$CH$_2$CH$_2$CH$_2$CH$_2$CH$_2$***C***H$_3$). (**Figure S1**, SI).

2.3. Preparation of polymer electrospun nanofibers

Nanofibers of 4-heptyl-1,2,3-triazole functionalized polysulfone (PSUT) were prepared by electrospinning polymer solutions with a standard syringe using a grounded rotating drum collector configuration (Linari Engineering) under ambient conditions. Fibers were collected onto a rotating drum with a rotation speed of 800 rpm and a translational speed of 10 mm s^{-1}. PSUT(30 mol%) and PSUT(90 mol%) nanofibers were obtained by electrospinning respectively a 13 wt% and 14 wt% polymer solution in anhydrous DMAc with an applied potential of 10 kV, a needle collector distance of 12 cm and a flow rate of 0.2 mL min^{-1}.

Non-modified polysulfone nanofibers were prepared by electrospinning a 18 wt% PSU solution in anhydrous dimethylacetamide (DMAc) and acetone in a 7:3 volume ratio as reported elsewhere[21].

2.4. Membrane preparation

2.4.1. Composite nanofiber membranes

Reinforced membranes embedding 12 wt% of fibers were prepared by impregnating electrospun webs with a 12 wt% dispersion of Aquivion® (equivalent weight, EW = 830 g eq^{-1}) in a mixture of water/propanol/DMAc (weight ratio: 38 %/47 %/3 %). A layer of Aquivion® dispersion was cast with a doctor blade. The electrospun web was then placed on the top of this layer and another layer of ionomer dispersion was cast onto it. Afterwards, the composite membrane was left to dry overnight at room temperature and then at 80 °C for 5h to remove remaining solvent. Membranes were hot pressed at 160 °C at 980.6 kPa for 15 min and then thermally treated at 160 °C for 45 min. After, these were first washed in 1 M H_2SO_4 for 1 h at 80 °C for the reactivation of sulfonic acid sites, then 4-5 times in Milli-Q water at room temperature until neutral pH was achieved, and finally in Milli-Q water at 80 °C for one hour. Membrane thicknesses of 50 and 30 µm were set respectively for *ex situ* and fuel cell characterization.

2.4.2. Non-reinforced Aquivion® membranes

A 16 wt% dispersion of Aquivion® (EW = 830 g eq^{-1}) in a mixture of water /propanol/DMAc (weight ratio: 50 %/24 %/10 %) was cast to obtain membranes of thickness similar to that of reinforced films. The membranes were left overnight at room temperature and then dried at 80 °C for 12h. Non-reinforced membranes were hot pressed, thermally treated and washed in the same way as for reinforced films.

2.5. Characterization of functionalized polymers

NMR spectra were recorded on a Bruker Avance HD 400 MHz spectrometer equipped with a BBFO (Broad Band Fluorine Observation) probe in DMF-d_6 using tetramethylsilane (TMS) as reference residual hydrogenated solvent.

2.6. Characterization of nanofiber webs and membranes

2.6.1. Reinforced membrane fiber content

The fiber content of the reinforced membranes was evaluated by the weight ratio between the web and the membrane after drying at 80 °C for 5h.

2.6.2. Fiber and membrane morphology

Morphology of electrospun nanofibers and membranes was analyzed by field emission-scanning electron microscopy (FE-SEM) using a Hitachi S-4800 microscope after coating with a Pt layer of few nanometers (≈ 2-3 nm) to provide electrical conductivity. Freeze-fractured membrane cross-sections were prepared by immersing and cutting samples in liquid

nitrogen. Fiber diameters were calculated using the ImageJ software. For each web, the dimension of more than 100 nanofibers was evaluated. A Gaussian function was used to fit the fiber diameter distribution of both PSUT(30 mol%) and PSUT(90 mol%) and to evaluate the average fiber diameter. TEM-EDX analysis of reinforced membrane cross-sections was carried out using a JEOL 2200FS (Source: FEG) microscope operating at 200 kV equipped with a CCD camera Gatan USC (16 MP). Quantitative EDX analysis was performed by evaluating the mass percentage of fluorine at different points between a region comprising only Aquivion® to a region with only nanofibers.

2.6.3. Membrane conductivity

Proton conductivity of the membranes was measured in-plane at 80 °C and 110 °C as a function of RH on 5 cm x 0.5 cm membrane strips in the frequency range 10 Hz–100 kHz with 100 mV signal amplitude by four-probe impedance measurements by using an Autolab, PGSTAT30 potentiostat/galvanostat equipped with a frequency response analysis module. The RH was controlled by using stainless steel sealed-off cells that comprise two communicating cylindrical compartments held at different temperatures, the cold compartment containing water, and the hot compartment housing the membrane under test. RH values were calculated from the ratio between the pressures of saturated water vapor (p) at the temperatures of the cold (Tc) and hot (Th) compartment:

$$RH\ (\%) = \left(\frac{\mathrm{p(Tc)}}{p(Th)}\right) * 100$$

2.6.4. Stress-strain tests

Stress-strain mechanical tests were performed by using a Zwick Roell Z1.0 instrument with a 200 N static load cell equipped with a climatic chamber that operated in the RH range of 30–95 % (± 0.5 %) and in the temperature range of 10-80 °C (± 0.5 °C). Measurements were performed on 100 mm x 5 mm film strips. Before the measurements at room temperature, samples were equilibrated for five days in vacuum desiccators at 53 % RH and RT (25 °C). The investigations at higher temperature and humidity were performed after sample equilibration in the climate chamber at 70 °C and 80 % RH for one day. An initial grip separation of 10.000 ± 0.002 mm and a crosshead speed of 30 mm min^{-1} were used. At least five replicate film strips were analyzed. The data were analyzed by the TestXpert V11.0 Master software and are presented as mean ± standard deviation (SD).

2.6.5. Membrane dimensional swelling in water

Gravimetric water uptake (WU, %) was determined by weighing the membranes after immersion in deionized water at 80 °C for 15 h (W_f) and then after drying them at 120 °C for 5 h (W_i). Before weighing, excess water was removed from the surface of hydrated samples by lightly pressing the membranes between two filter papers. Membrane water uptake was calculated using the following relationship:

$$\mathrm{WU}\ (\%) = \left(\frac{\mathrm{Wf} - \mathrm{Wi}}{\mathrm{Wi}}\right) * 100$$

Dimensional swelling in water was determined by measuring the dimensions of rectangular samples of membrane after immersion in liquid water at 80 °C for 15 h as well as after drying at 120 °C for 5 h. The dimensional change was calculated using the following equation:

$$(\%) = \left(\frac{\mathrm{Dw} - \mathrm{Dd}}{\mathrm{Dd}}\right) * 100$$

where Dw and Dd are the dimensions (volume, area or thickness) of respectively the wet and dry sample.

2.6.6. Membrane ion exchange capacity

The ion exchange capacity (IEC) of the membranes was determined by acid-base titrations by using a Radiometer automatic titrimeter (TIM900 TitraLab and ABU91 Burette) operating with the equilibrium point method. Before titration, the membranes were heated at 120 °C for 5 h to remove water and determine the weight of the dried sample. The dry membranes were equilibrated overnight at RT with a 0.1 M NaCl aqueous solution to exchange Na^+ ions with the membrane protons. The solutions were then titrated with 0.1 M NaOH without removing the membranes [9].

2.6.7. Membrane permeability

Permeation measurements were performed using a fuel cell test station with the membranes under evaluation held in a single fuel cell fixture (active surface area of 8 cm^2) equipped with a micro GC, gas flow mixer and pressure monitor. The membranes were placed in the single cell hardware, gas sealed at 1 bar and conditioned to ensure equilibrium state of the ionomer. The hydrogen permeability was determined at 80 % relative humidity at 80 °C.

2.6.8. Fuel cell polarization curve measurements and durability tests

I-V curves were recorded on membrane electrode assemblies (MEAs) (8 cm^2) prepared by incorporating the proton exchange membrane between two electrodes (Sigracet 10BC from Baltic Fuel Cells, nominal platinum loading of 0.5 mg_{Pt} cm^{-2}) and two propylene sub-gaskets. MEAs were hot-pressed at 160 °C and 6.3 MPa for 3 minutes. Prior to measurements, MEAs were conditioned in the fuel cell at 80 °C, 100 % RH and 2.5 bar absolute pressure for at least 12 hours, at a current density of 400 mA cm^{-2} until constant potential was obtained. I-V curves were recorded on a Bio-Logic VMP3B-80 A booster. The fuel cell was fed with H_2 and air using a constant flux of 150 and 500 mil min^{-1}, respectively. Accelerated stress test (AST) were performed on MEAs based on reinforced and non-reinforced Aquivion® membranes using standard 25 cm^2 single cell hardware in FuelCon fuel cell station. Baltic Fuel Cells electrodes with a nominal loading of 0.2 mg_{Pt} cm^{-2} (anode) and 0.5 mg_{Pt} cm^{-2} (cathode) were used in this study. Break-in procedure consisted of cycling operation at 0.4 V and 0.8 V for 5 min for 4 hours at 80 °C and 100 % RH in H_2/air. After break-in, MEAs were exposed to wet/dry cycling between 0 and 100 % RH in 10-minute cycles. Durability testing was performed at OCV at 90 °C in H_2/air with gas flow rates of 420 and 1450 sccm respectively.

3. Results and Discussion

3.1. Electrospun polymer nanofibers

Electrospinning of 4-heptyl-1,2,3-triazole-functionalized polysulfone afforded regular and homogenous nanofibers with thin diameter and small size distribution. Thin nanofibers are indeed advantageous due to their high surface area ensuring enhanced polymer/ionomer interface. For this study, triazole functionalized polysulfone with a degree of functionalization of 30 mol% (PSUT(30 mol%)) and 90 mol% (PSUT(90 mol%)) functional group per repeat unit were taken into consideration which allowed the effect of the amount of interfacial triazole moieties on membrane properties to be investigated. In **Figure 1** are depicted the SEM micrographs of fiber webs of non-functionalized (PSU) and functionalized polysulfone prepared with the optimized electrospinning conditions, as well as the histograms of the related fiber diameter distribution.

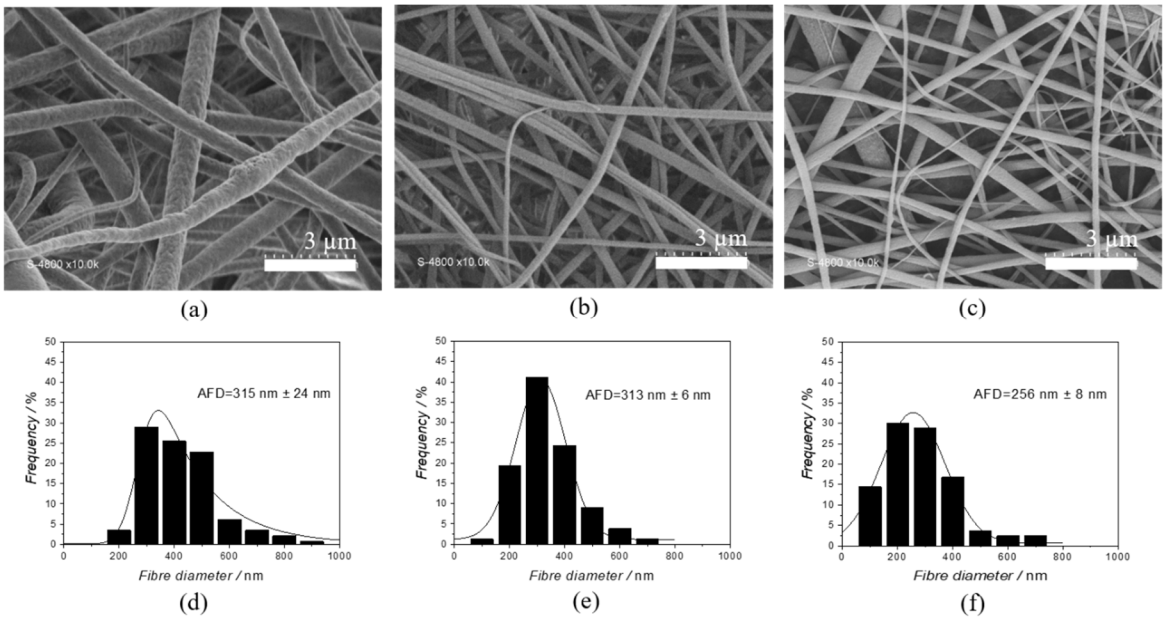

Figure. 1. FE-SEM micrographs of electrospun nanofibers of PSU (a), PSUT(30 mol%) (b) and PSUT(90 mol%) (c) selected to be incorporated into the Aquivion® matrix. Histograms of fiber diameter distribution of PSU (d), PSUT(30 mol%) (e) and PSUT(90 mol%) (f).

Randomly oriented and non-welded nanofibers were obtained in all cases. This web morphology was targeted since it ensures a strengthening of the membrane throughout its thickness. In particular, the absence of fiber welding allows the web to expand during its impregnation with the PFSA dispersion leading to a homogeneous membrane architecture[21]. Diameters of PSUT(30 mol%) **(Figure 1 e)** and PSUT(90 mol%) **(Figure 1 f)** fibers range from 100 to 700 nm with an average fiber diameter (AFD) of 313 ± 6 nm and 256 nm ± 8 nm respectively. Thus, the degree of functionalization seems to have a negligible effect on the nanofiber morphology. Nonetheless, a higher proportion of thin nanofibers (diameter *ca.* 100 nm) was obtained for the triazole functionalized polysulfone with the higher degree of substitution. In comparison, PSU fiber diameters range from 200 to 900 with AFD of 390 nm (**Figure 1 d**). The difference in diameter can be ascribed to the different electrospinning conditions (18 wt% solution of the non-functionalized polymer in a in DMAc/acetone (7v/3v) binary solvent system[21], while PSUT was electrospun at lower concentration (13-14 wt%) and in pure DMAc).

3.2. Membrane morphology

In the subsequent step, the electrospun webs of functionalized and pristine polysulfone were used to prepare reinforced membranes by impregnation with Aquivion® (EW = 830 g eq^{-1}). In

this study, fiber content was fixed at 12 wt%. Membranes reinforced by triazole functionalized polysulfone are referred to as Aq-PSUT(n) where n is the degree of functionalization of PSUT. For comparison, non-reinforced Aquivion® and Aquivion-PSU nanofiber reinforced membranes are labelled as Aq and Aq-PSU respectively. In **Figure 2** are represented the SEM images of cross-sections of membranes reinforced with functionalized and non-functionalized PSU fiber webs.

In all cases, fully dense and crack-free films were obtained, indicating that PFSA impregnation was successful. Moreover, both the ionomer and the nanofibers are homogenously distributed throughout membrane cross-section.

In the present study, a clear difference emerges between membranes reinforced with the functionalized and the non-functionalized polysulfone fibers that may be seen in the higher magnification micrographs of **Figure 2**. For the non-functionalized PSU/Aquivion® membrane a void space is observed between the fibers and the surrounding ionomer (**Figure 2 d**). This might be a result of the freeze-fracture process during preparation of samples for SEM or of the drying of the membrane under vacuum conditions of the analysis.

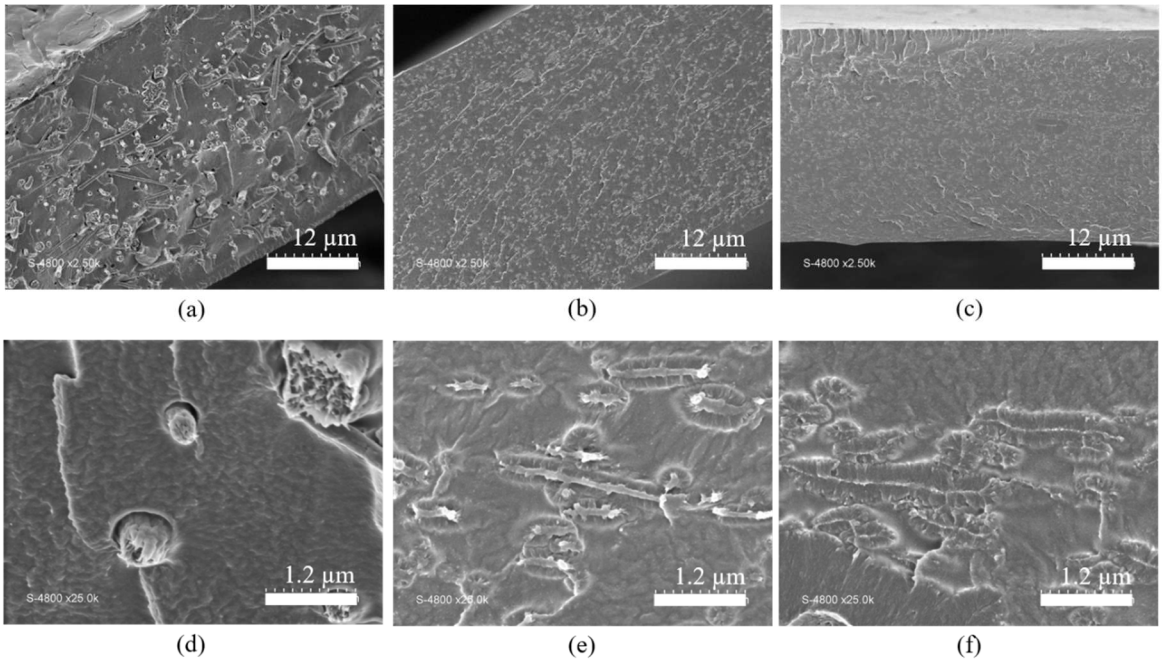

Figure. 2. SEM micrographs of freeze-fractured cross-sections of Aq-PSU (a,d), Aq-PSUT(30 mol%) (b,e) and Aq-PSUT(90 mol%) (c,f).

In contrast, under the same measurement conditions, Aquivion® appears to be in tight contact with the triazole functionalized polymer fibers, with the appearance of a halo around

the PSUT fibers, suggesting the possible formation of a blend region with interpenetration of ionomer and PSUT fibers (**Figure 2 e, f** and **Figure 3**).

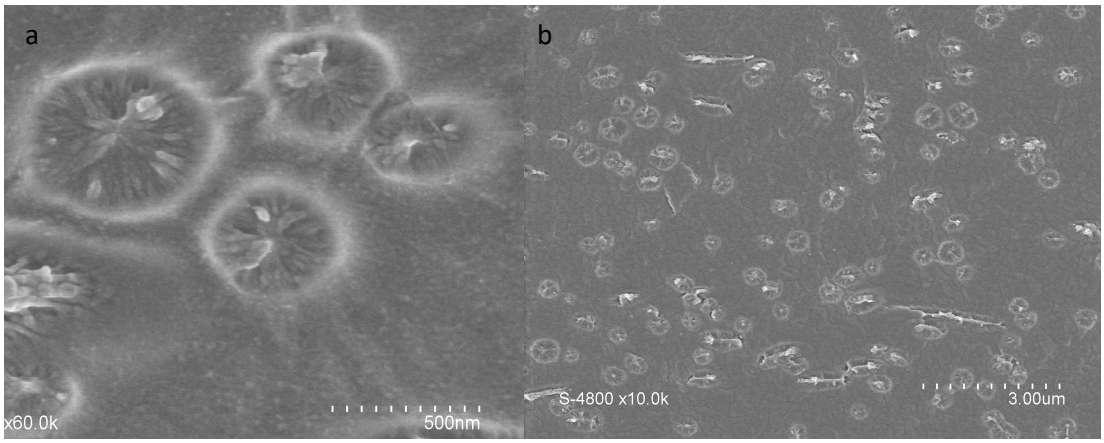

Figure 3. SEM micrographs at different magnifications of the cross-section of the composite membrane Aq-PSUT (30 mol%).

These results give a preliminary corroboration of the presence of acid-base ionic cross-linking between 1,2,3-triazole moieties on the functionalized polymer fibers and sulfonic acid sites of the Aquivion® matrix, unlike for polysulfone fibers.

This could be promoted by PFSA/PSUT co-penetration during the membrane hot-pressing procedure at temperature higher than the glass transition temperature (T_g)[39] and the α transition temperature of Aquivion® (≈ 125 °C)[1]. Quantitative TEM-EDX analysis shed further information on the PFSA/PSUT blend region at the fiber/ionomer interface (**Figure 4**). Using fluorine as a marker to evaluate the penetration of Aquivion® into the fiber, it is observed that for Aq-PSU the fluorine signal sharply decreases to almost 0 mass% at the fiber edge **(Fig. 4 a** and **b)** However, for Aq-PSUT, a gradual transition is observed with a signal from fluorine persisting even inside the fiber **(Fig. 4 c** and **d),** consistent with an Aquivion®/PSUT(30 mol%) blend region at the PFSA/fiber interface. It is known that hydrogen bonds can enhance the miscibility of otherwise immiscible blends.[43]

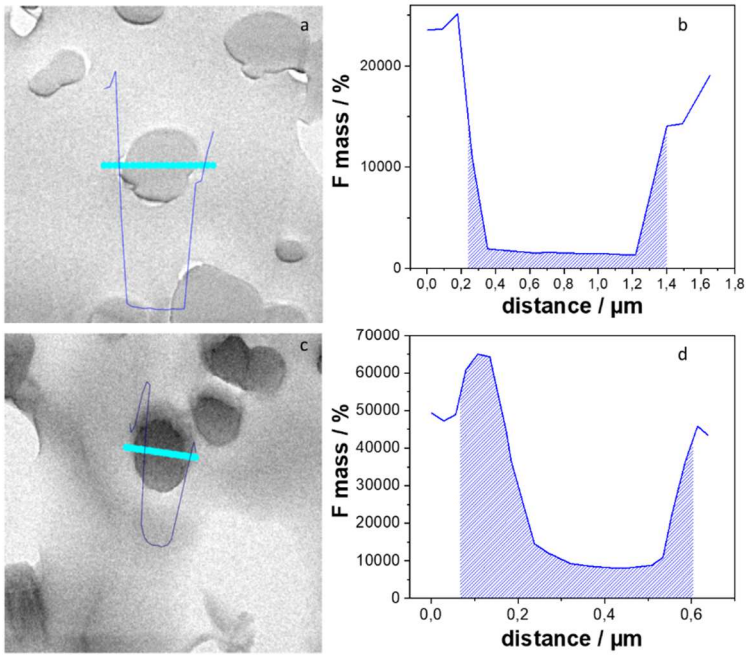

Figure 4. TEM micrograph of the Aq-PSU (a) of the Aq-PSUT(30 mol%) (c) and the related fluorine mass distribution (b, d). On TEM micrographs are indicated the analyzed region (diameter of the nanofiber, light blue line) and the corresponding fluorine mass distribution (blue line).

3.3. Membrane proton conductivity

The in-plane proton conductivity of membranes as a function of relative humidity at 80 °C and 110 °C is shown respectively in **Figure 5 a** and **b.**

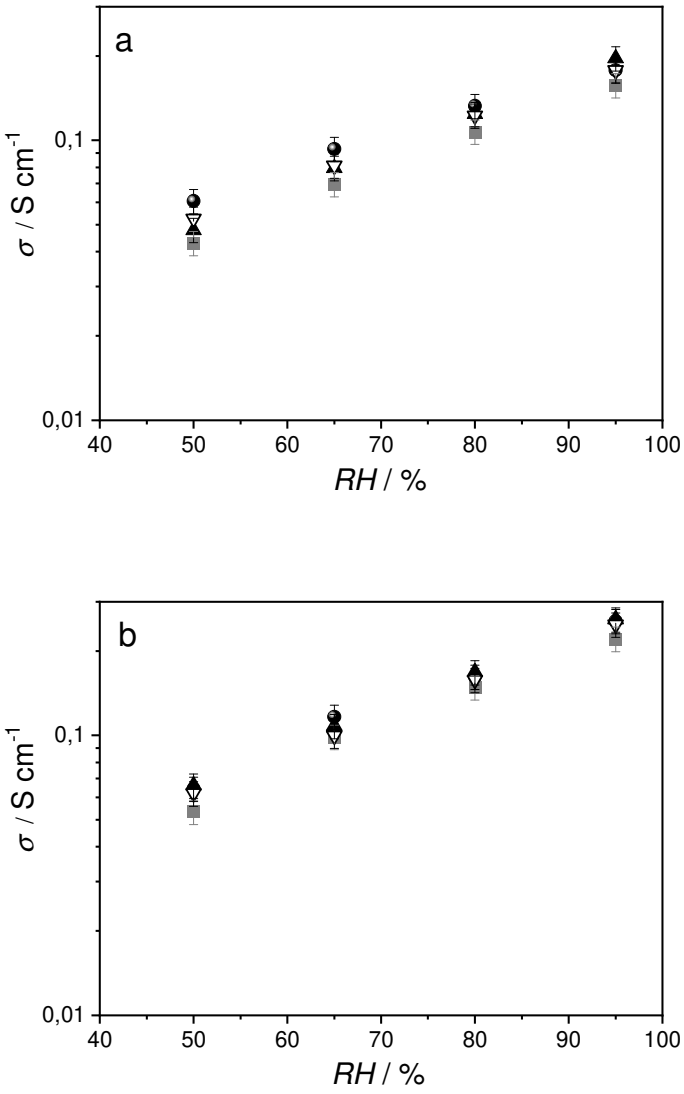

Figure 5. In-plane proton conductivity as a function of RH at 80 °C (a), and 110 °C (b) of Aq ( ), Aq-PSU (!), Aq-PSUT(30 mol%)(7) and Aq-PSUT(90 mol%)(X).

The proton conductivity of all the reinforced and non-reinforced membranes increases with temperature and relative humidity as expected for PFSA[11,44,45]. The conductivity of non-reinforced Aquivion® extends from 60 mS cm^{-1} (50 % RH) to 180 mS cm^{-1} (95 % RH) at 80 °C and reached 260 mS cm^{-1} at 95 % RH and 110 °C. The presence of PSU nanofibers leads to a slight decrease of the conductivity of the pure ionomer in agreement with the reduction of the concentration of proton carriers due to the presence of the non-conducting reinforcement[18,21]. Some loss in conductivity could be expected upon the introduction of triazole functionalized polysulfone nanofiber reinforcement, due to possible proton transfer from sulfonic acid groups in their interaction with basic groups of the fiber surface. No such conductivity reduction was observed however, and indeed there is negligible effect of the

degree of functionalization. This implies that protons are not immobilized and still available for transport.

Experimental ion exchange capacity (IEC) of composite membranes reinforced with functionalized polysulfone were determined and compared to those of Aq-PSU and Aq830 (**Table 1**)

Table 1. Experimental ion exchange capacity (IEC) values of Aquivion® and reinforced membranes with 12 wt% fiber content.

Membrane	**IEC (mequiv·g^{-1})**
Aq830	1.17
Aq-PSU	1.01
Aq-PSUT(30 mol%)	0.98
Aq-PSUT(90 mol%)	1.02

The IEC of reinforced membranes is slightly lower than that of pristine Aquivion® (*ca* 15 % lower IEC for 12 wt% of inert polymer fiber content). Independently of their degree of functionalization, Aq-PSUT reinforced membranes have the same IEC as Aq-PSU membranes, around 1 mequiv·g^{-1}. These results are in agreement with proton conductivity determined from in-plane measurements for the different membranes. On the contrary, in acid-base blend of triazole-functionalized polymer and sulfonated ionomer IEC values are lower than the theoretical values calculated assuming that only the ionomer provides dissociable protons[38]. The IEC values obtained for the nanocomposite membranes could be explained considering that the interaction does not involve all triazole moieties, but only those at the extended Aquivion®/PFSA interface. This assumption is supported by the fact that the degree of functionalisation of the PSU (30-90 mol% triazole) does not seem to play a significant role in the properties of the corresponding fiber reinforced membranes.

3.4. Mechanical properties

The mechanical properties of reinforced functionalized and non-functionalized polysulfone membranes were determined at 20 °C and 45 % RH and at 70 ºC and 80 % RH. The obtained results are summarized in **Table 2** and stress-strain curves are presented in **Figure S2** (Supporting Information).

Table 2. Mechanical properties of reinforced and non-reinforced membranes at 20 °C and 45 % RH and at 70 °C and 80 % RH.

Membrane	Young modulus, E ($N \cdot mm^{-2}$)		Yield stress ($N \cdot mm^{-2}$)		Breaking strength ($N \cdot mm^{-2}$)		Elongation at break, ε (%)		Modulus of toughness, MT (N·mm)	
	20°C-45%RH	70°C-80%RH	20°C-45%RH	70°C-80%RH	20°C-45%RH	70°C-80%RH	20°C-45%RH	70°C-80RH%	20°C-45%RH	70°C-80%RH
Aq	196±7	107±9	10±2	5±1	11±1	6±1	54±2	81±3	500±9	439±18
Aq-PSU	349±4	203±10	/	/	15±1	9±1	9.9±1.3	11.0±2.0	125±7	51±3
Aq-PSUT(30 mol%)	390±10	259±5	18±1	11±2	20±1	13±1	135±19	164±11	2853±25	1891±11
Aq-PSUT(90 mol%)	385±14	220±18	17±1	9±1	18±1	10±1	59±19	89±30	1274±12	643±8

All reinforced membranes presented a significantly higher Young modulus (E) than reference Aquivion® due to the presence of the fiber reinforcement. Elastic modulus followed the order Aq-PSUT(30 mol%)>Aq-PSUT(90 mol%)>Aq-PSU>Aq and decreased with the increase in temperature-relative humidity as expected for PFSA based membranes[1]. At 70 °C and 80 % RH the membrane reinforced with PSUT(30 mol%) nanofibers displayed a Young modulus of 259 $N \cdot mm^{-2}$, the membrane reinforced with PSU, 203 $N \cdot mm^{-2}$, and the non-reinforced Aquivion®, 107 $N \cdot mm^{-2}$. The higher stiffness of triazole functionalized PSU reinforced membranes with respect to Aq-PSU can be explained by ionic interactions made possible by the presence of triazole moieties. This effect became more remarkable at higher temperature and RH confirming the effectiveness of the functionalized fibers in enhancing membrane mechanical strength in conditions similar to those of actual fuel cell operation. Moreover, Aq-PSUT(30 mol%) presented Young modulus higher than Aq-PSUT(90 mol%): 390 $N \cdot mm^{-2}$ *vs.* 385 $N \cdot mm^{-2}$ at RT, and 259 $N \cdot mm^{-2}$ *vs.* 220 $N \cdot mm^{-2}$ at 70 °C and 80 % RH. This could be related to a lower mechanical strength of the PSUT(90 mol%) with respect to the PSUT(30 mol%). We previously reported[39] that an increase in the degree of 4-heptyl-1,2,3-triazole functionalization on PSU resulted in a decrease in glass transition temperature

(T_g =138 °C for PSUT(30 mol%) *vs* T_g =115 °C for PSUT(90 mol%), which is related to the crystallinity and therefore to the mechanical strength.

Both yield stress and breaking strength followed the same trend of the elastic modulus, and decreased by increasing temperature and relative humidity. Modulus of toughness (MT) was also estimated in order to quantify energy absorption capability of the membrane before breaking, and it followed the sequence: Aq-PSUT(30 mol%)>Aq-PSUT(90 mol%)>Aq>Aq-PSU. This result further confirmed the strength of the interaction between the ionomer and the PSUT nanofibers and the efficacy of the latter as mechanical reinforcement. No clear trend is observed in the mechanical properties, going from Aq-PSUT (30 mol%) to Aq-PSUT (90 mol%). This, combined with the proton conductivity results, suggests that the increase in the functionalization degree of the polymer does not increase the interaction between fibers and Aquivion®, which is consistent with this interaction involving only the region at the fiber/ionomer interface.

We can conclude that Aq-PSUT(30 mol%) presented the highest strength of the membranes investigated (non-reinforced, reinforced with PSU and PSUT (90 mol%)). Furthermore, its properties are much improved over those of the non-reinforced membranes at 70 °C/80 %RH than at ambient conditions.

3.5. Membrane dimensional water swelling

The dimensional change of reinforced and non-reinforced membranes from a dry to a water-swollen state is reported in **Table 3**. Lower water uptake and volumetric water swelling was observed for all the composite membranes in comparison to non-reinforced Aquivion®. Membranes reinforced with functionalized polysulfone fibers undergo less change in dimension than the PSU reinforced membranes. This behavior is, once again, attributed to the ionic interactions taking place between the sulfonic acid sites of the PFSA and the 1,2,3-triazole moieties of PSUT(30 mol%) and PSUT(90 mol%) fibers, resulting in an improved dimensional stability limiting membrane water uptake.

Table 3. Water uptake (WU) and dimensional water swelling of pristine Aquivion® membrane and PSU and functionalized PSUT reinforced Aquivion® membranes between dry and swollen states in liquid water at 80 °C for 15h.

Membrane	WU (%)	Volume swelling (%)	Area swelling (%)	Thickness swelling (%)
Aq	73±3	121±4	81±3	22±4
Aq-PSU	53±3	91±4	18±2	61±4
Aq-PSUT(30 mol%)	45±3	77±4	15±2	54±4
Aq-PSUT(90 mol%)	48±3	83±4	26±2	45±4

The dimensional change of all fiber reinforced membranes is markedly anisotropic, with remarkably lower in-plane (area) variation and higher through-plane (thickness) variation compared to non-reinforced Aquivion®. For instance, Aq-PSUT(30 mol%), Aq-PSUT(90 mol%) and Aq-PSU have area swelling of respectively 15 %, 26 % and 18 % while for the non-reinforced Aquivion®, the area swelling is 81 %. Aquivion® presents the lowest thickness swelling (22 %), against 61% for Aq-PSU, 54 % for Aq-PSUT(30 mol%) and 45 % for Aq-PSUT(90 mol%). Moreover, the area swelling was observed to be isotropic in all reinforced membranes (same increase in sample length and width), indicating uniform in-plane reinforcing effect of the fibers. The electrospun web thus constrains the ionomer towards swelling in the through-plane direction, due to the in-plane fiber directionality and the weak through-plane fiber interconnectivity[18,21]. Area stresses are considered predominant and one of the main cause of premature membrane mechanical failure[4]. Further reduction in area swelling is desirable, and this can be achieved increasing the amount of electrospun nanofibers in the membrane over the 12 wt% of this work. In-plane membrane dimensional stabilization is thus considered crucial and a significantly enhanced lifetime has been reported for reinforced membranes thanks to lower in-plane swelling and enhanced mechanical strength[20].

Aq-PSUT(30 mol%) displayed the best combination of mechanical strength and ductility, dimensional stability and proton conductivity and was selected for integration into a membrane electrode assembly (MEA) and single fuel cell tests.

3.6. Membrane permeability

The hydrogen permeation values measured for Aq, Aq-PSU and Aq-PSUT(30 mol%) were as follows 2.4 x 10^{-13} mol/s cm kPa, 2.1 x 10^{-13} mol/s cm kPa and 1.6 x 10^{-13} mol/s cm kPa. It can be concluded that the presence of the reinforcement decreased membrane permeability. Furthermore, PSUT nanofibers proved to be an efficient barrier to hydrogen, the corresponding membranes demonstrating the lowest hydrogen permeation. In order to confirm the high performance of PSUT reinforcement in membrane durability enhancement the pristine and composite membranes were subjected to wet dry cycling at OCV.

3.7. Fuel cell polarization curves and durability

I-V curves of membrane electrode assemblies (MEAs) with membranes of Aq, Aq-PSU and Aq-PSUT(30 mol%) of thickness 30±1 µm, at 80 ºC, 100 % RH and 2.5 bar absolute (H_2/air) are reported in **Figure 6 a**. In all cases, high OCV, with similar values ranging between 0.936 for Aq and 0.947 V for Aq-PSUT(30 mol%) were obtained. This indicates excellent gas barrier properties for all membranes. Moreover, similar polarization curves were obtained to ca. 0.6 A cm^{-2} for all MEAs as expected from the similar membrane proton conductivity described above, with differences in the mass transport region at higher current density, leading to maximum power densities of Aq, 0.56 W cm^{-2} with non-reinforced Aquivion®, 0.52 W cm^{-2} with Aq-PSUT(30 mol%), and 0.48 W cm^{-2} with Aq-PSU.

The MEAs incorporating the reinforced and non-reinforced membranes were subjected to an accelerated ageing test protocol designed to combine chemical and mechanical degradation by performing wet-dry cycles while holding at OCV[46]. The voltage decay with time was recorded (**Figure 6**). A membrane exposed to repeated shrinking-swelling cycles eventually loses its mechanical integrity, while the free radicals produced at open circuit voltage attack the ionomer and cause chemical degradation according to pathways that are now well understood [47].

The pristine Aquivion® membrane demonstrated a lifetime of only 75 hours before the voltage dropped abruptly due to pinhole formation in the membrane. For the MEA based on PSU reinforced membrane the lifetime was 250 hours. In contrast, the voltage - time profile of the MEA with the Aq-PSUT(30 mol%) membrane is quite different and shows no evidence for a catastrophic event indicating end of life.

The durability test was stopped at 450 hours. The black curve in **Figure 6 b**, corresponding to the MEA based on PSUT reinforced Aquivion®, is an end of test result, not end of life, the membrane not showing significant degradation or failure after 450 hours. We can highlight that such membrane did not incorporate any radical scavenger and suggest the role of triazole functionalities of the fibrous reinforcement in chemically stabilizing the membrane to radical attack.

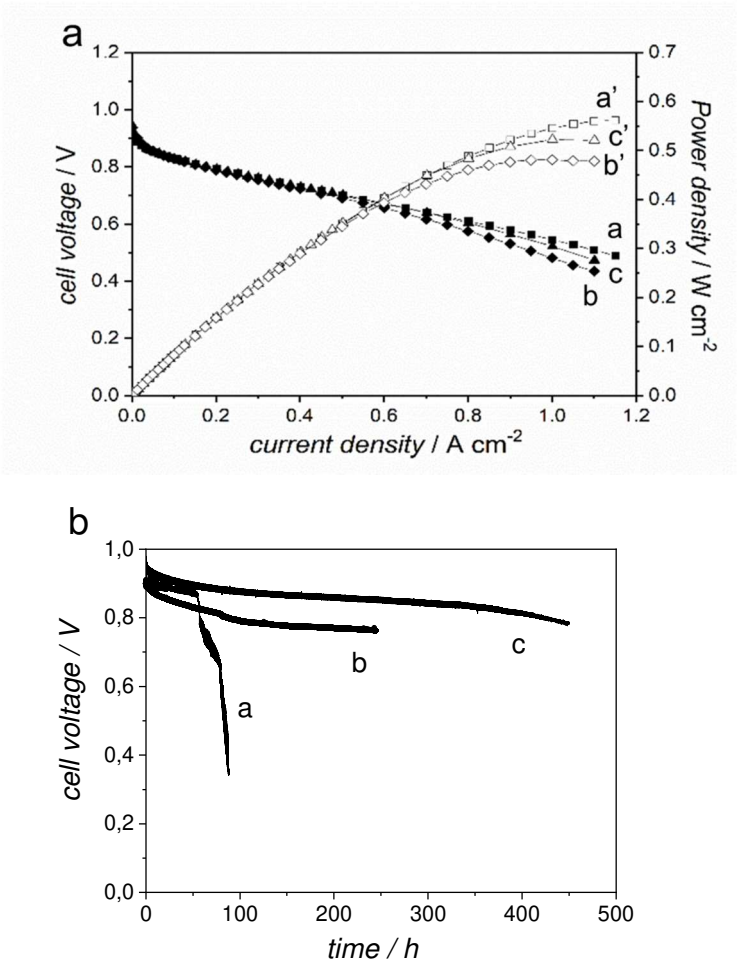

Figure 6. a) Polarization curves of MEAs with membranes Aq (■, a), Aq-PSU (♦, b) and Aq-PSUT(30 mol%) (▲, c) at 80 ºC, 100 % RH and 2.5 bar abs (H_2/air), and corresponding power density Aq(□, a'), Aq-PSU(◊, b') and Aq-PSUT(30 mol%) (Δ, c'); b) OCV hold at 90 °C as a function of time for MEAs incorporating PSUT(30 mol%) nanofiber reinforced Aquivion® (c), PSU reinforced Aquivion® (b), non-reinforced Aquivion® membrane (a).

4. Conclusion

This work demonstrated the effect of an active reinforcement, *i.e.* nanofibers interacting by hydrogen bond or ionic crosslinking with the ionomer, on mechanical properties and durability of proton exchange membranes. The reinforcement based on 4-heptyl-1,2,3-triazole functionalized PSU nanofibers resulted in a remarkable improvement in membrane mechanical strength and dimensional stability with respect to non-reinforced Aquivion® and Aquivion® reinforced by non-functionalized polysulfone nanofibers. The interaction at the fiber/ionomer interface between triazole (fiber) and -SO_3H (ionomer), evidence for which was obtained from electron microscopy observation of a local polymer blend-like region, might be at the origin of this improved properties set. The proton conductivity of triazole functionalized PSU Aquivion® membranes is closely similar to that of non-reinforced Aquivion®. The significantly greater MEA durability enabled by the use of the Aq-PSUT(30 mol%) membrane (in the absence of any radical scavenging component) affords new possibilities for further improving fuel cell performance by reducing the membrane thickness. This work demonstrates the flexible approach of active fibrous reinforcement to achieve highly conducting, dimensionally stable and durable fuel cell membranes, with applications too in other energy conversion devices (electrolyzers), and opens up a range of perspectives on tuning the fiber/ionomer interface.

Acknowledgements: The research leading to these results has received funding from the European Research Council under the European Union's Seventh Framework Programme (FP/2007-2013)/ERC Grant Agreement n. 306682. SC acknowledges the financial support from the French IUF.

References

[1] A. Kusoglu, A.Z. Weber, New Insights into Perfluorinated Sulfonic-Acid Ionomers, Chem. Rev. 117 (2017) 987–1104. doi:10.1021/acs.chemrev.6b00159.

[2] M. Zatoń, S. Cavaliere, D.J. Jones, J. Rozière, Design of Heterogeneities and Interfaces with Nanofibers in Fuel Cell Membranes BT - Handbook of Nanofibers, in: A. Barhoum, M. Bechelany, A. Makhlouf (Eds.), Handb. Nanofibers, Springer International Publishing, Cham, 2018: pp. 1–37. doi:10.1007/978-3-319-42789-8_32-1.

[3] S. Subianto, M. Pica, M. Casciola, P. Cojocaru, L. Merlo, G. Hards, et al., Physical and chemical modification routes leading to improved mechanical properties of perfluorosulfonic acid membranes for PEM fuel cells, J. Power Sources. 233 (2013) 216–230. doi:10.1016/j.jpowsour.2012.12.121.

[4] D. Qiu, L. Peng, X. Lai, M. Ni, W. Lehnert, Mechanical failure and mitigation strategies for the membrane in a proton exchange membrane fuel cell, Renew. Sustain. Energy Rev. 113 (2019) 109289. doi:10.1016/j.rser.2019.109289.

[5] B. Bahar, A.R. Hobson, J.A. Kolde, D. Zuckerbrod, B. Bahar, A.R. Hobson, J.A. Kolde, D. Zuckerbrod, Ultra-thin integral composite membrane, US 5547551, 1996. https://www.google.ch/patents/US5547551.

[6] P. Xiao, J. Li, H. Tang, Z. Wang, M. Pan, Physically stable and high performance Aquivion/ePTFE composite membrane for high temperature fuel cell application, J. Membr. Sci. 442 (2013) 65–71. doi:10.1016/j.memsci.2013.04.014.

[7] Y. Tang, A. Kusoglu, A.M. Karlsson, M.H. Santare, S. Cleghorn, W.B. Johnson,

Mechanical properties of a reinforced composite polymer electrolyte membrane and its simulated performance in PEM fuel cells, J. Power Sources. 175 (2008) 817–825. doi:10.1016/j.jpowsour.2007.09.093.

[8] B. Shoibal, P. David N., F. Simon, Advances in Proton Exchange Membrane Technology, ECS Trans. 50 (2012) 887–895.

[9] M. Casciola, P. Cojocaru, A. Donnadio, S. Giancola, L. Merlo, Y. Nedellec, et al., Zirconium phosphate reinforced short side chain perflurosulfonic acid membranes for medium temperature proton exchange membrane fuel cell application, J. Power Sources. 262 (2014) 407–413. doi:10.1016/j.jpowsour.2014.04.010.

[10] A. Donnadio, M. Pica, S. Subianto, D.J. Jones, P. Cojocaru, M. Casciola, Promising Aquivion Composite Membranes based on Fluoroalkyl Zirconium Phosphate for Fuel Cell Applications, ChemSusChem. 7 (2014) 2176–2184.

[11] A. Donnadio, M. Pica, A. Carbone, I. Gatto, T. Posati, G. Mariangeloni, et al., Double filler reinforced ionomers: a new approach to the design of composite membranes for fuel cell applications, J. Mater. Chem. A. 3 (2015) 23530–23538. doi:10.1039/C5TA07917A.

[12] G. Alberti, R. Narducci, M.L. Di Vona, S. Giancola, Annealing of Nafion 1100 in the Presence of an Annealing Agent: A Powerful Method for Increasing Ionomer Working Temperature in PEMFCs, Fuel Cells. 13 (2013) 42–47. doi:10.1002/fuce.201200126.

[13] S. Giancola, R.A.B. Arciniegas, A. Fahs, J.-F. Chailan, M.L. Di Vona, P. Knauth, et al., Study of Annealed Aquivion® Ionomers with the INCA Method, Membranes (Basel). 9 (2019) 134. doi:10.3390/membranes9100134.

[14] S. Cavaliere, M. Zatoń, F. Farina, D. Jones, J. Rozière, Electrospun Materials for Proton Exchange Membrane Fuel Cells and Water Electrolysis, in: E. Kny, K. Ghosal, S. Thomas (Eds.), Electrospinning From Basic Res. to Commer., Royal Society of Chemistry, 2018: pp. 205–237.

[15] S. Subianto, S. Giancola, G. Ercolano, Y. Nabil, D. Jones, J. Rozière, et al., Electrospun Nanofibers for Low-Temperature Proton Exchange Membrane Fuel Cells, in: S. Cavaliere (Ed.), Electrospinning Adv. Energy Environ. Appl., CRC Press, Boca Raton, 2015: pp. 29–60. doi:10.1201/b18838-3.

[16] R. Sood, S. Cavaliere, D.J. Jones, J. Rozière, Electrospun nanofibre composite polymer

electrolyte fuel cell and electrolysis membranes, Nano Energy. 26 (2016) 729–745. doi:10.1016/j.nanoen.2016.06.027.

[17] C. Boaretti, L. Pasquini, R. Sood, S. Giancola, A. Donnadio, M. Roso, et al., Mechanically stable nanofibrous sPEEK/Aquivion® composite membranes for fuel cell applications, J. Membr. Sci. 545 (2018) 66–74. doi:10.1016/j.memsci.2017.09.055.

[18] J.B. Ballengee, P.N. Pintauro, Composite Fuel Cell Membranes from Dual-Nanofiber Electrospun Mats, Macromolecules. 44 (2011) 7307–7314. doi:10.1021/ma201684j.

[19] J. Choi, K.M.K. Lee, R. Wycisk, P.N. Pintauro, P.T. Mather, Nanofiber network ion-exchange membranes, Macromolecules. 41 (2008) 4569–4572. doi:10.1021/ma800551w.

[20] D. Powers, R. Wycisk, P.N. Pintauro, Electrospun tri-layer membranes for H2/Air fuel cells, J. Membr. Sci. 573 (2019) 107–116. doi:10.1016/j.memsci.2018.11.046.

[21] S. Giancola, M. Zatoń, Á. Reyes-Carmona, M. Dupont, A. Donnadio, S. Cavaliere, et al., Composite short side chain PFSA membranes for PEM water electrolysis, J. Membr. Sci. 570–571 (2019) 69–76. doi:10.1016/j.memsci.2018.09.063.

[22] J. Wang, Y. He, L. Zhao, Y. Li, S. Cao, B. Zhang, et al., Enhanced proton conductivities of nanofibrous composite membranes enabled by acid–base pairs under hydrated and anhydrous conditions, J. Membr. Sci. 482 (2015) 1–12. doi:10.1016/j.memsci.2015.02.015.

[23] Y. He, H. Zhang, Y. Li, J. Wang, L. Ma, W. Zhang, et al., Synergistic proton transfer through nanofibrous composite membranes by suitably combining proton carriers from the nanofiber mat and pore-filling matrix, J. Mater. Chem. A. 3 (2015) 21832–21841. doi:10.1039/C5TA03601A.

[24] J. Wang, P. Li, Y. Zhang, Y. Liu, W. Wu, J. Liu, Porous Nafion nanofiber composite membrane with vertical pathways for efficient through-plane proton conduction, J. Membr. Sci. 585 (2019) 157–165. doi:10.1016/j.memsci.2019.05.041.

[25] D. Jones, J. Rozière, S. Cavaliere, S. Subianto, S. Burton, Reinforced ionomer membranes, fabrication and application in energy conversion devices, WO2016020668, 2016. https://patents.google.com/patent/WO2016020668A1/en.

[26] L. Wang, N. Deng, G. Wang, J. Ju, B. Cheng, W. Kang, Constructing Amino-Functionalized Flower-Like MOFs Nanofibers in Sulfonated Poly(ether sulfone)

Proton Exchange Membrane for Simultaneously Enhancing Interface Compatibility and Proton Conduction, ACS Appl. Mater. Interfaces. (2019). doi:10.1021/acsami.9b13496.

[27] V. V. Rostovtsev, L.G. Green, V. V. Fokin, K.B. Sharpless, A Stepwise Huisgen Cycloaddition Process: Copper(I)-Catalyzed Regioselective "Ligation" of Azides and Terminal Alkynes, Angew. Chemie Int. Ed. 41 (2002) 2596–2599. doi:10.1002/1521-3773(20020715)41:14<2596::AID-ANIE2596>3.0.CO;2-4.

[28] C.W. Tornøe, C. Christensen, M. Meldal, Peptidotriazoles on Solid Phase: [1,2,3]-Triazoles by Regiospecific Copper(I)-Catalyzed 1,3-Dipolar Cycloadditions of Terminal Alkynes to Azides, J. Org. Chem. 67 (2002) 3057–3064. doi:10.1021/jo011148j.

[29] J.-F. Lutz, 1,3-Dipolar Cycloadditions of Azides and Alkynes: A Universal Ligation Tool in Polymer and Materials Science, Angew. Chemie Int. Ed. 46 (2007) 1018–1025. doi:10.1002/anie.200604050.

[30] B.P. Mudraboyina, M.M. Obadia, I. Allaoua, R. Sood, A. Serghei, E. Drockenmuller, 1,2,3-Triazolium-based poly(ionic liquid)s with enhanced ion conducting properties obtained through a click chemistry polyaddition strategy, Chem. Mater. 26 (2014) 1720–1726. doi:10.1021/cm500021z.

[31] R. Sood, M.M. Obadia, B.P. Mudraboyina, B. Zhang, A. Serghei, J. Bernard, et al., 1,2,3-Triazolium-based poly(acrylate ionic liquid)s, Polymer (Guildf). 55 (2014) 3314–3319. doi:10.1016/j.polymer.2014.04.017.

[32] R. Sood, B. Zhang, A. Serghei, J. Bernard, E. Drockenmuller, Triethylene glycol-based poly(1,2,3-triazolium acrylate)s with enhanced ionic conductivity, Polym. Chem. 6 (2015) 3521–3528. doi:10.1039/C5PY00273G.

[33] U. Akbey, S. Granados-Focil, E.B. Coughlin, R. Graf, H.W. Spiess, 1H Solid-State NMR Investigation of Structure and Dynamics of Anhydrous Proton Conducting Triazole-Functionalized Siloxane Polymers, J. Phys. Chem. B. 113 (2009) 9151–9160. doi:10.1021/jp9030909.

[34] J.A. Johnson, M.G. Finn, J.T. Koberstein, N.J. Turro, Construction of Linear Polymers, Dendrimers, Networks, and Other Polymeric Architectures by Copper-Catalyzed Azide-Alkyne Cyclo- addition "Click" Chemistry, Macromol. Rapid Commun. 29

(2008) 1052−1072.

[35] M.K. Ahn, B. Lee, J. Jang, C.M. Min, S. Bin Lee, C. Pak, et al., Facile preparation of blend proton exchange membranes with highly sulfonated poly(arylene ether) and poly(arylene ether sulfone) bearing dense triazoles, J. Membr. Sci. 560 (2018) 58–66. doi:10.1016/j.memsci.2018.05.011.

[36] U. Sen, A. Bozkurt, A. Ata, Nafion/poly(1-vinyl-1,2,4-triazole) blends as proton conducting membranes for polymer electrolyte membrane fuel cells, J. Power Sources. 195 (2010) 7720–7726. doi:10.1016/j.jpowsour.2010.04.087.

[37] B. Yue, G. Zeng, Y. Zhang, S. Tao, X. Zhang, L. Yan, Improved performance of acid-base composite of phosphonic acid functionalized polysulfone and triazolyl functionalized polysulfone for PEM fuel cells, Solid State Ionics. 300 (2017) 10–17. doi:10.1016/j.ssi.2016.11.011.

[38] W. Li, A. Manthiram, M.D. Guiver, Acid–base blend membranes consisting of sulfonated poly(ether ether ketone) and 5-amino-benzotriazole tethered polysulfone for DMFC, J. Membr. Sci. 362 (2010) 289–297. doi:10.1016/j.memsci.2010.06.059.

[39] R. Sood, A. Donnadio, S. Giancola, A. Kreisz, D.J.D.J. Jones, S. Cavaliere, 1,2,3-Triazole-Functionalized Polysulfone Synthesis through Microwave-Assisted Copper-Catalyzed Click Chemistry: A Highly Proton Conducting High Temperature Membrane, ACS Appl. Mater. Interfaces. 8 (2016) 16897–16906. doi:10.1021/acsami.6b02713.

[40] R.J. Thibault, K. Takizawa, P. Lowenheilm, B. Helms, J.L. Mynar, J.M.J. Fréchet, et al., A versatile new monomer family: Functionalized 4-vinyl-1,2,3-triazoles via click chemistry, J. Am. Chem. Soc. 128 (2006) 12084–12085. doi:10.1021/ja0648209.

[41] R.K. Iha, K.L. Wooley, A.M. Nyström, D.J. Burke, M.J. Kade, C.J. Hawker, Applications of Orthogonal "Click" Chemistries in the Synthesis of Functional Soft Materials, Chem. Rev. 109 (2009) 5620–5686. doi:10.1021/cr900138t.

[42] N. Dubey, M.C. Sharma, A. Kumar, P. Sharma, A click chemistry strategy to synthesize geraniol-coupled 1,4-disubstituted 1,2,3-triazoles and exploration of their microbicidal and antioxidant potential with molecular docking profile, Med. Chem. Res. (2015) 1–15. doi:10.1007/s00044-015-1329-5.

[43] S.W. Kuo, Hydrogen-bonding in polymer blends, J. Polym. Res. 15 (2008) 459–486.

doi:10.1007/s10965-008-9192-4.

[44] S. Subianto, A. Donnadio, S. Cavaliere, M. Pica, M. Casciola, D.J. Jones, et al., Reactive coaxial electrospinning of ZrP/ZrO2 nanofibres, J. Mater. Chem. A. 2 (2014) 13359–13365. doi:10.1039/c4ta01383b.

[45] D.J. Jones, Membrane materials and technology for low temperature fuel cells, in: C. Hartning, C. Roth (Eds.), Polym. Electrolyte Membr. Direct Methanol Fuel Cell Technol., Woodhead Publishing Limited, 2012.

[46] R. Mukundan, A.M. Baker, A. Kusoglu, P. Beattie, S. Knights, A.Z. Weber, et al., Membrane Accelerated Stress Test Development for Polymer Electrolyte Fuel Cell Durability Validated Using Field and Drive Cycle Testing, J. Electrochem. Soc. 165 (2018) F3085–F3093. doi:10.1149/2.0101806jes.

[47] M. Zatoń, J. Rozière, D.J. Jones, Current understanding of chemical degradation mechanisms of perfluorosulfonic acid membranes and their mitigation strategies: a review, Sustain. Energy Fuels. 1 (2017) 409–438. doi:10.1039/C7SE00038C.

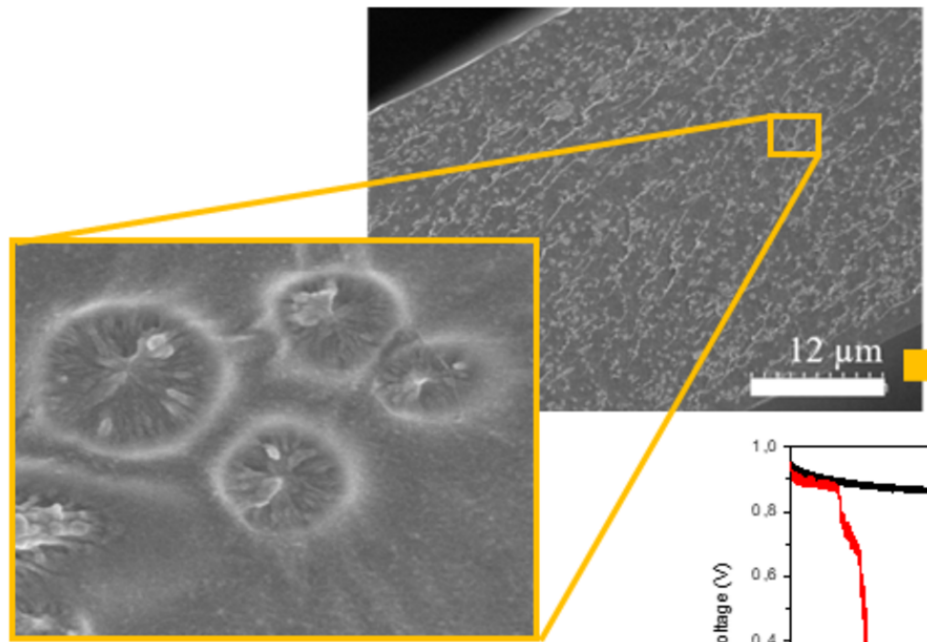

Ionic crosslinking between fibers and ionomer for enhanced membrane durability